Indian Journal of Pure & Applied Physics
Vol. 60, November 2022, pp. 922-932
DOI: 10.56042/ijpap.v60i11.63930

Synthesis, Computational, FT- IR, NMR and UV-Vis Spectral Studies of Bioactive 2-(4-fluorophenyl)-4-(4-(4-methoxyphenyl)-5-(3-nitrophenyl)-4H-1,2, 4-triazol-3-yl)quinoline

Shraddha Shukla, Anil Kumar Verma, Abha Bishnoi*, Poornima Devi & Sonam Rai
Department of Chemistry, Lucknow University, Lucknow 226 007, India

Received 19 June 2022; accepted 20 October 2022

The work describes synthesis of a bioactive molecule 2-(4-fluorophenyl)-4-(4-(4-methoxyphenyl)-5-(3-nitrophenyl)-4H-1, 2, 4-triazol-3-yl)quinoline. The characterization has been done with the help of various spectroscopic techniques followed by *in-silico* studies including various structural parameters viz. electrostatic potential, electrophilicity (ω), chemical potential (μ), chemical hardness (η), thermodynamic properties at various temperatures, Natural bond orbital (NBO), Non-linear optical (NLO), electric dipole moment, polarizability and first static hyperpolarizability. Reactivity descriptors were also investigated to find out the sites liable for electrophilic and nucleophilic attack. The compound was also bio-evaluated for its antimicrobial and antioxidant activity. It showed significant activity against *S. typhi* and a positive antioxidant activity shown by reduction in color with percentage inhibition of 89%.

Keywords: Spectroscopic; Hyperpolarizability; Electrophilicity; Electrostatic; Thermodynamics

1 Introduction

The DFT studies predict material behaviour of the molecules on the basis of quantum mechanical considerations, thus they support the experimental chemistry[1-4]. Density Functional Theory creates a platform to study the structure of chosen compound. 2-(4-fluorophenyl)-4-(4-(4-methoxyphenyl)-5-(3-nitrophenyl)-4H-1,2,4-triazol-3-yl)quinoline became the subject of interest for the authors as it is evident from literature that high nitrogen content heterocycles are therapeutically significant due to their wide range of biological activities[5-6]. In this regard, azoles have been shown a constant interest as more than hundred azole derivatives have been used as drugs[7-8]. Triazoles[9] and their fused heterocyclic derivatives are considered to be pharmacologically important due to their biological activities such as antibacterial[10-12], antifungal[13-14], antitumor[15], anti-inflammatory[16], anti-tubercular[17], hypoglycaemic[18-19], anti-depressant[20]. Literature survey revealed that no spectroscopic, computational and biological studies have been performed on the title compound so far. Therefore, this work presents synthesis, biological evaluation and *in silico* studies for the title molecule 2-(4-fluorophenyl)-4-(4-(4-methoxyphenyl)-5-(3-nitrophenyl)-4H-1,2,4-triazol-3-yl)quinoline.

*Corresponding authors: (Email: abhabishnoi5@gmail.com)

2 Computational details

To ascertain the theoretical-experimental consistency quantum chemical calculations were performed. All the quantum details were computed with the help of Density Functional Theory with B3LYP/6-31G (d, p) method using Gaussian 09W program package[21] with the default convergence criteria without any constraint on the geometry[22]. The NBO calculations[23] were carried out at DFT/B3LYP level to predict various second order interactions. The Time Dependent Density Functional Theory (TD-DFT) at B3LYP/6-31-G (d, p) level in DMSO as a solvent by using IEFPCM model available in Gaussian software was used for Frontier orbitals analysis and electronic absorption spectra of the optimized molecule. Molecular electrostatic potential surface (MESP) studies depicted the positive and negative charged electrostatic potentials in the molecule.

3 Results and discussion

The reaction sequenced for the title compound is illustrated in Scheme 1.The target compound **(3)** with a triazole core was synthesized in two steps. The first step is the synthesis of 2-(4-fluorophenyl)-N-(4-methoxyphenyl)quinoline-4-carboxamide **(2)** by refluxing a mixture of 2-(4-fluorophenyl)-quinoline-4-carboxylic acid **(1)**, methoxy aniline and

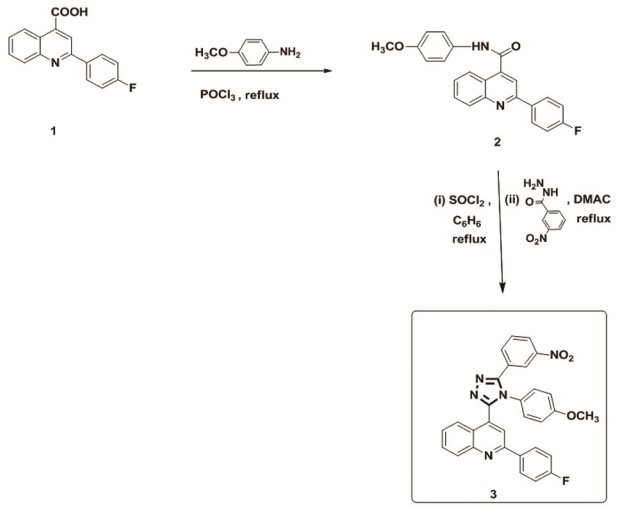

Scheme 1

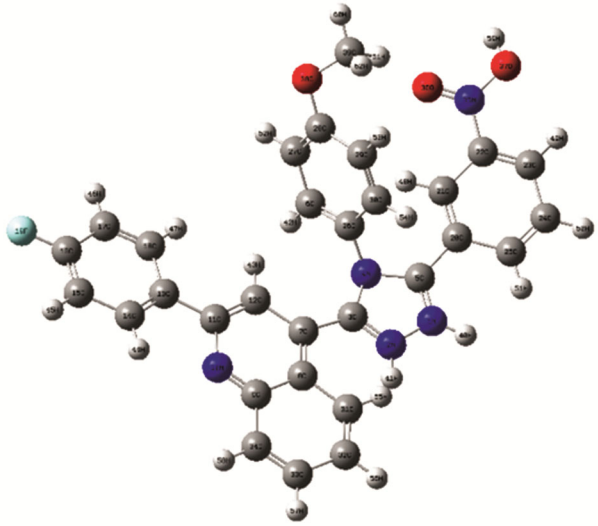

Fig. 1 — Optimized Structure of title compound

phosphorus oxychloride. The second step was carried out with (4-fluorophenyl)-N-(4-methoxyphenyl) quinoline-4-carbimidoyl chloride and 3-nitrobenzohydrazide using DMAC. Structure of the compound was confirmed by recording its IR, ^{1}H NMR, ^{13}C NMR and mass spectra. The structure of (3) was in good agreement with its spectroscopic data.

3.1 Materials and Method

Melting points were determined in a melting point apparatus.^{1}H and ^{13}C-NMR spectra were recorded on a Bruker 400 MHz instrument. Chemical shifts were measured in DMSO-d_6 with TMS as internal reference and chemical shift values were imparted in ppm. Abbreviations for data quoted are: s, singlet; d, doublet; t, triplet; m, multiplet. An IR spectrum of compound was recorded as KBr pellets on a Perkin-Elmer Fourier transform infra-red spectrophotometer. Ultraviolet spectrum was recorded in the region 200-500 nm on UV-visible Double-Beam Spectrophotometer (systronic-2203) instrument with DMSO as a solvent.

Procedure for the synthesis of 2-(4-fluorophenyl)-N-(4-methoxyphenyl)quinoline-4-carboxamide (2)

A mixture of 2-(4-fluorophenyl)-quinoline-4-carboxylic acid **(1)** (0.01 mol)[24-26], methoxy aniline (0.01 mol) and phosphorus oxychloride (10 mL) was heated, then poured onto crushed ice. The solid mass formed was collected and washed with sodium bicarbonate solution (5%) followed with water and dried. Recrystallization was done from a mixture of ethanol and dimethyl formamide (2:1).Yield: ~78%; R_f: 0.85; (40% Hexane:EA)

Procedure for the synthesis of 2-(4-fluorophenyl)-4-(4-(4-methoxyphenyl)-5-(3-nitrophenyl)-4H-1,2,4-triazol-3-yl)quinolone (3)

A solution of 0.01 mol 2-(4-fluorophenyl)-N-(4-methoxyphenyl)quinoline-4-carbimidoyl chloride, obtained by refluxing (2) and thionyl chloride in dry benzene for 8 hrs. It was refluxed with 3-nitrobenzohydrazide in DMAC for ~10 hrs to yield (3) a reddish brown semi-solid. The crude product was recrystallized with ethanol and dimethyl formamide (2:1). The TLCs were obtained using Chloroform: Methanol and Hexane: EA (v/v) as mobile phase. Yield: ~73%; R_f: 0.82; (40% Hexane:EA); IR (KBr) cm^{-1} : 3266 (=C-H), 3038 (-C-H), 1531 (-C=C-), 1622 & 1407 ($NO_{2\ asym}$ & $_{sym}$), 1350 (C-O), 1253 (C-F) ^{1}H NMR (DMSO-D_6, 300 MHz) δ (ppm): 7.19-7.21 (d, 2H), 7.54-7.56 (d, 2H), 7.79-7.83 (m, 5H), 8.41-8.45 (m, 4H), 8.61-8.94 (m, 4H), 3.90(s, 1H); ^{13}C NMR ($CDCl_3$, 75 MHz) δ (ppm):55.46, 114.63, 115.16, 123.46, 123.66, 124.64, 126.64, 126.80, 127.13, 127.46, 127.82, 128.09, 130.80, 137.79, 141.53, 148, 150.30, 154.27, 156.89, 158.52, 163.35; ESI-MS: m/z 518 $[M+1]^{+}$, Calculated (m/z)=517.

3.2 Molecular Geometry

Bond lengths & bond angles, obtained as optimised structural parameters for the title compound are presented in Table S1. Fig. 1 shows the optimised structure displaying the atom numbers of the investigated molecule. Marked changes in several features such as electronic and spectroscopic are possible due to a small change in the geometry of the

molecules[27]. Thus it was essential to examine the optimized geometry of the studied molecule (**3**). The geometric parameters of (3) are predicted very well with little distortions. Most of the C-C and C-H bond distances of aromatic rings are found to be in the range of 1.39-1.44 and 1.08-1.085 Å respectively. The theoretical values for C-N, C-O and N-O varied from 1.35-1.43, 1.34-1.43 and 1.24-1.38 Å respectively. The bond length value for C-F was found to be 1.39 Å. The variations in bond lengths and bond angles in the molecule can be explained on the basis of presence of lone pair of electrons, electro negativity of the central atom, conjugation present in it and various other intermolecular interactions[28].

3.3 Spectral Characterization

Gauge Independent Atomic Orbital (GIAO) approach was employed to calculate ^{1}H and ^{13}C NMR chemical shifts by DFT using B3LYP method at 6-31-G (d, p) as basis set[29]. Experimental and theoretical ^{1}H and ^{13}C NMR chemical shifts of the title compound have been reported in Table 1(a). Fig. 2 depicting the correlation graph between the calculated and experimental values, followed the

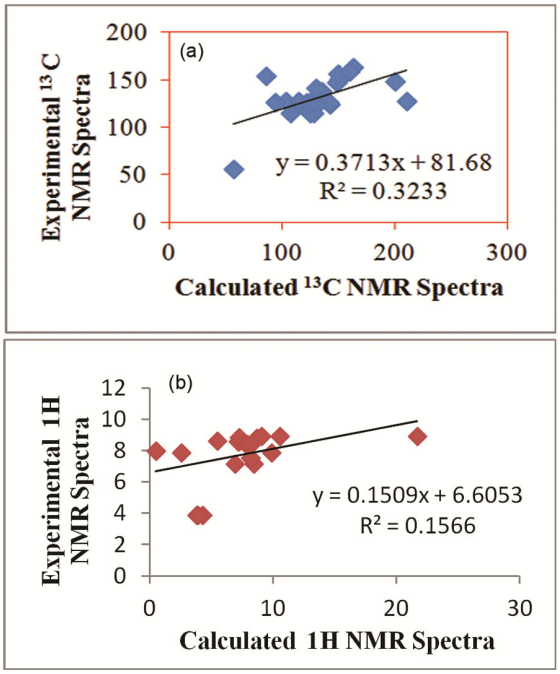

Fig. 2 — Correlation graph between (a) experimental and calculated 13C NMR chemical shifts and between (b) experimental and calculated 1HNMR chemical shifts using B3LYP 6-31G (d, p).

Table 1(a) — Experimental and calculated ^{13}C NMR and ^{1}H NMR chemical shifts of title compound using DFT/B3LYP 6-31G (d,p).

Atom no.	Calculated	Experimental	Atom no.	Calculated	Experimental
3C	86.435	154.27	40H	11.672	8.94
5C	150.9412	150.3	41H	10.523	8.94
6C	122.063	126.64	42H	8.13	7.54
7C	135.6205	137.79	43H	5.4602	8.64
8C	122.787	123.46	44H	8.6701	8.83
9C	148.555	147.53	45H	7.2301	8.61
11C	149.5202	156.89	46H	7.131	8.61
12C	142.5655	123.66	47H	7.2413	8.85
13C	132.3868	130.8	48H	0.4882	8
14C	128.3298	128.09	49H	0.5118	8.01
15C	115.1461	124.64	50H	2.54	7.87
16C	163.09	163.35	51H	9.87	7.87
17C	114.68	124.64	52H	8.43	7.19
18C	125.967	128.09	53H	6.8804	7.19
20C	210.9394	127.46	54H	8.2	7.53
21C	103.0749	127.82	55H	7.7931	8.41
22C	200.9716	148	56H	7.9103	8.4
23C	114.9598	127.13	57H	7.9231	8.43
24C	142.1069	126.8	58H	8.2225	8.45
25C	94.0069	126.8	59H	9.0275	8.93
26C	125.68	114.63	60H	4.2779	3.9
27C	128.7822	115.16	61H	3.7928	3.9
28C	160.7378	158.52	62H	3.8702	3.9
29C	107.1751	115.16			
30C	125.2464	126.64			
31C	124.1504	124.64			
32C	131.4718	124.64			
33C	128.3123	126.64			
34C	130.8705	141.53			
39C	57.1361	55.46			

linear equations, for ^{1}H NMR and for 13C NMR where 'x' and 'y' are experimental and calculated ^{1}H and ^{13}C NMR chemical shifts respectively. The experimental ^{1}H and ^{13}C NMR spectra are given in supplementary Fig. S1 and S2. The recorded (FT-IR) and computed vibrational wavenumbers by B3LYP/6-31G (d, p) are given in Table 1(b). Calculated wave numbers were compared with experimental wavenumbers after being scaled down by a factor 0.9679 for B3LYP. The value of correlation coefficient (R2= 0.994 using B3LYP) depicted an excellent compliance between experimental and calculated wave numbers. Fig. 3 contains the correlation graph (correlation coefficient R2= 0.994 using B3LYP) between experimental and calculated wavenumbers and experimental and calculated FT–IR spectra are presented in Fig. S3 and Fig. 4 respectively. The results indicated a good agreement between experimental and theoretical values. Computational data revealed that all aromatic hydrogens appeared in the range of δ 7.13-9.02 which showed agreement with the experimental values ranging from δ 7.19-8.94. The methoxy hydrogens appeared at δ 3.87-4.27 which matched well with the experimental value at δ 3.90. The calculated ^{13}C shifts for C5 at δ 150.94 matched well with experimental shift at 150.30 pertaining to carbon present in triazole nucleus. Also the vibrational bands ascertained in the FT-IR spectrum have wave numbers lying in the expected range. In the FT-IR spectra of the C-F stretching vibrations appeared at 1253.89 cm^{-1} and 1296.4 cm^{-1} as experimental and theoretical values respectively. The other significant vibrations were found for C-O-C stretching at 1350.51 cm^{-1} (experimental) and 1365.43 cm^{-1} (theoretical) respectively and for N-O stretching at 1622.96 cm^{-1} and 1645.97 cm^{-1} as experimental and theoretical IR vibrations.

Table 1(b) — Experimental and calculated FT-IR vibrations of title compound using DFT/B3LYP 6-31G (d,p).

Calculated	Experimental B3LYP	Vibrational Assignment
764.96	756.08	CH bending
1365.43	1350.51	C-O-C stretching
1174.37	1159.72	CH streching
1296.4	1253.89	C-F stretching
1333.1	1407.04	N-O stretching
1532.06	1531.75	C=C stretching
1645.97	1622.96	N-O stretching
3014.69	3038.22	CH streching
3196.68	3080.69	=CH stretching
3227.64	3266.3	=CH stretching

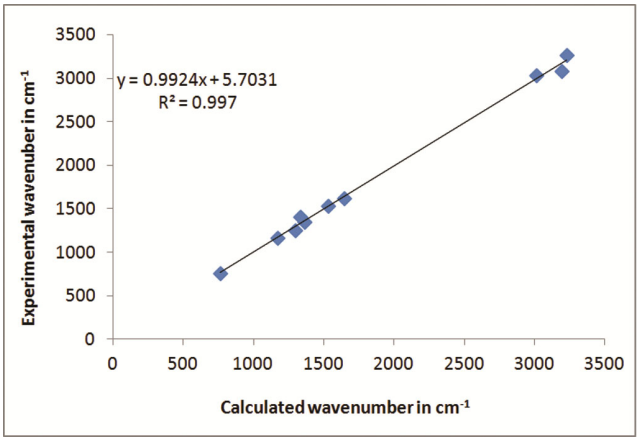

Fig. 3 — Correlation graph between experimental and calculated wavenumbers using B3LYP /6-31G

3.4 UV-Visible Absorption Spectroscopy

An analysis of the electron density of highest occupied molecular orbitals (HOMO) and lowest unoccupied molecular orbitals (LUMO) of the title compound gives an idea about the ground and excited state electron transfer processes. UV-Visible spectrum was studied with the help of DFT calculations at B3LYP/6-31G (d, p) level. Table 2 contains the oscillator strengths (*f*), percentage contribution of probable transitions and corresponding absorption wavelengths. Fig. 5 represents the experimental UV spectra. Fig. 6 contains the HOMO-LUMO energy gap diagram involved in electronic transistions within the molecule. HOMO-LUMO distribution gives an insight into the reactive properties of the title molecule. UV-Visible spectrum showed strong π →π*

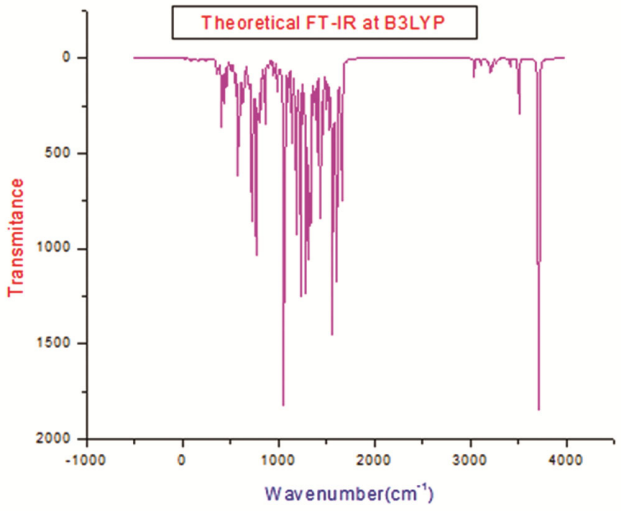

Fig. 4 — Theoretical IR spectra of title compound

Table 2 — Experimental and theoretical absorption wavelength λ (nm), excitation energies E (eV) of title compound using B3LYP functional and 6-31-G/ (d, p) basis set.

S. No.	Major contributing Molecular orbitals	E (eV)	Calculated (λ_{max})	Oscillatory strength (f) B3LYP	Assignment	Observed (λ_{max})
1	H→L +5 (66%)	2.9710	417	0.0017	π →π*	348
2	H-2→L (65%)	2.8083	441	0.0584	π → π*	305
3	H-2→L+2 (64%)	3.6527	339	0.0633	π → π*	248
4	H-9→L (66%)	3.6433	340	0.0040	π →π*	225
5	H-5→L (62%)	3.5739	346	0.0263	π →π*	205

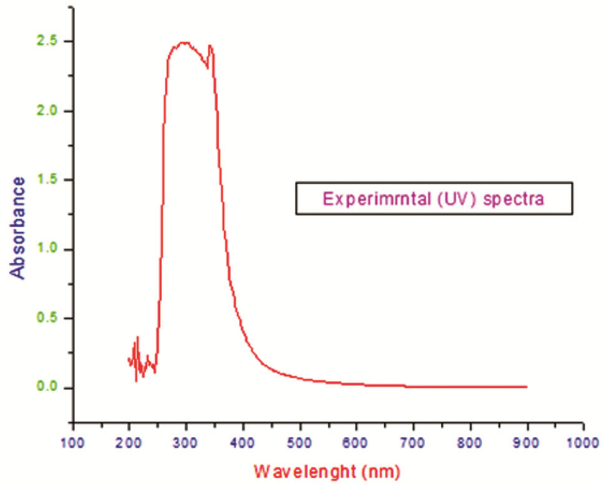

Fig. 5 — Experimental UV-Vis spectrum of title compound

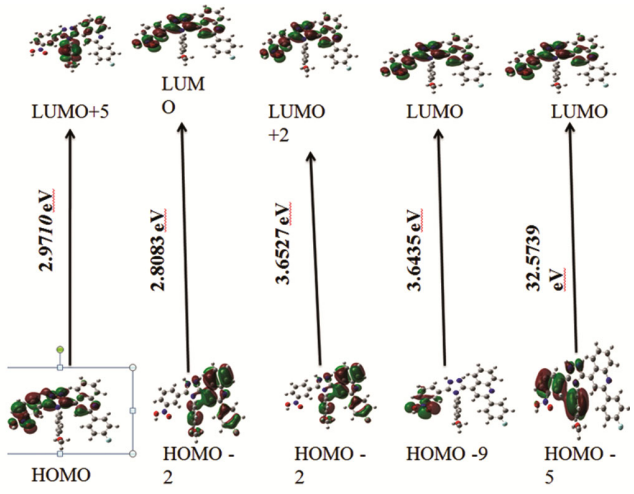

Fig. 6 — HOMO-LUMO energy gap diagram involved in electronic transitions in isolated (gaseous)phase of the title compound

electronic transition at 417 nm from H→L+5 (*f*=0.0017) with percentage contribution of 66% and energy gap of 2.9170 ev, π →π* transistion at 441 nm from H-2→L (*f*=0.0584) with percentage contribution of 65% and energy gap of 2.8083 ev, π →π* transistion at 339 nm from H-2→L-2 (*f*=0.0633) with

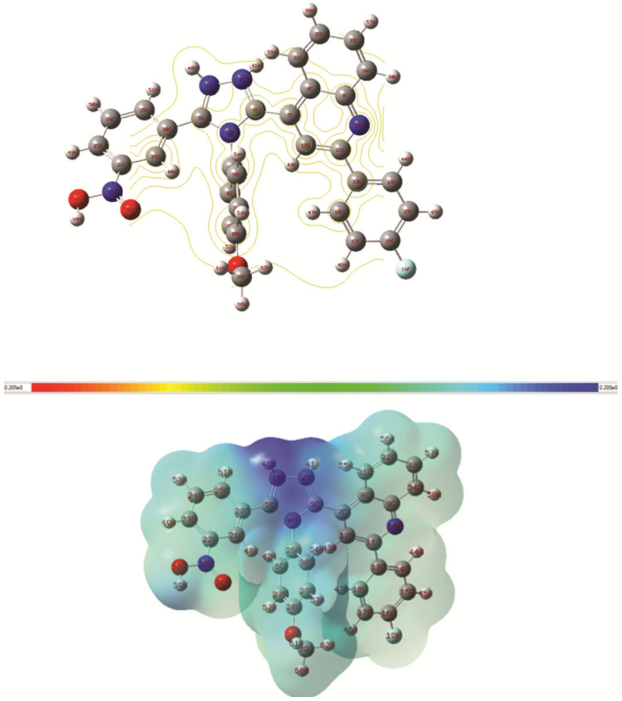

Fig. 7 — 3D and 2D plots of the molecular electrostatic potential of title molecule

a percentage contribution of 64% and energy gap of 3.6527 ev, π →π* transistion at 340 from H-9→L (*f*=0.0040) with a percentage contribution of 66% and energy gap of 3.6435 ev

respectively. Another π →π* transition at 346 nm was observed from H-5→L (*f*=0.0243). The observed values for transistions H→L+5, H-2→L, H-2→L-2, H-9→L and H-5→L were found at 348 nm, 305nm, 248 nm, 225 nm, and 205 nm respectively. The values obtained for the HOMO-LUMO energy gap suggest the relative stability of the title compound.

3.5 Molecular Electrostatic Potential

Molecular electrostatic potential (MEP) approach can be effectively employed to study the potentially reactive sites for nucleophilic and electrophilic attack[30]. MEP sketch representing the chemically active sites and comparative reactivity of atoms[31] is shown in Fig. 7. Electrophilic reactivity is represented

by the negative (red) region, nucleophilic reactivity by the positive (blue) region and zero potential region of MEP by green colour. The decrease in electrostatic potential is seen from red < orange < yellow < green < blue. The MESP map revealed that the region of maximum positive electrostatic potential is situated around N1, N2 and N4 with MEP value around +0.205 a.u. (blue region) pertaining to nucleophilic reactivity.

3.6 Natural Bond Orbital Analysis

NBO is a conducive method for the exploration of charge transfer or conjugative interactions in molecular system. Along with this, it also provides information about interactions in both filled and virtual orbital spaces that could enhance the analysis of intra and intermolecular interactions. The Natural Bond Analysis (NBO)[32] has been performed using Gaussian 09 package at the B3LYP/6-31G(d, p) method. The extent of conjugation increases due to greater interaction between electron donors and acceptors as per the increase in stabilisation energy value. Analysis of interaction between donor level and acceptor level bonds was done with the help of second order Fock matrix[33]. NBO analysis is tabulated in Table 3. Higher the stabilization energy values, more intense would be the interaction between electron donors and acceptors. As per NBO analysis,

Table 3 — Second order perturbation theory analysis of Fock matrix in NBO basis of the title compound

Donor (i)	Type	Ed/e	Acceptor (i)	Type	Ed/e	E(2)a	E(j)a-E(i)b	F(I,j)c
BD(2)C6-N27	σ	1.707	BD*(2)C26-C30	π*	0.415	17.58	0.27	0.063
BD(2)C6-N27	σ	1.707	BD*(2)C28-C29	π*	0.377	20.26	0.28	0.07
BD(2)C7-C12	π	1.688	LP(1)C8	n	1.025	35.17	0.16	0.084
BD(2)C7-C12	π	1.688	LP*(1)C11	n	0.928	38.08	0.17	0.09
BD(2)C7-C12	π	1.688	BD*(2)C3-N4	σ*	0.643	28.53	0.17	0.07
BD(2)C9-N10	σ	1.621	LP(1)C8	n	1.025	29.49	0.16	0.08
BD(2)C9-N10	σ	1.621	LP*(1)C11	n	0.928	66.02	0.18	0.113
BD(2)C13-C18	π	1.649	BD*(2)C14-C15	π*	0.298	20.21	0.29	0.07
BD(2)C13-C18	π	1.649	BD*(2)C16-C17	π*	0.37	18.43	0.28	0.064
BD(2)C14-C15	π	1.673	BD*(2)C13-C18	π*	0.392	18.03	0.28	0.064
BD(2)C14-C15	π	1.673	BD*(2)C16-C17	π*	0.37	24.06	0.27	0.073
BD(2)C16-C17	π	1.636	BD*(2)C13-C18	π*	0.37	22.32	0.29	0.072
BD(2)C16-C17	π	1.636	BD*(2)C14-C15	π*	0.298	16.91	0.3	0.064
BD(2)C20-C21	π	1.613	LP(1)C5	n	1.125	79.45	0.09	0.091
BD(2)C20-C21	π	1.613	LP(1)C25	n	1.123	40.33	0.16	0.09
BD(2)C20-C21	π	1.613	BD*(1)C22-N35	σ*	0.056	24.88	0.21	0.07
BD(1)C20-C25	π	1.967	BD*(1)N4-C5	σ*	0.036	5.58	1.1	0.07
BD(2)C22-N35	σ	1.706	BD*(2)C20-C21	π*	0.351	12.77	0.38	0.063
BD(2)C22-N35	σ	1.706	BD*(2)C22-N35	σ*	0.722	5.3	0.31	0.041
BD(2)C22-N35	σ	1.706	BD*(2)C23-C24	π*	0.301	7.15	0.42	0.049
BD(2)C23-C24	π	1.717	LP(1)C25	n	1.123	38.34	0.13	0.083
BD(2)C23-C24	π	1.717	BD*(2)C22-N35	σ*	0.722	35.16	0.18	0.08
BD(2)C26-C30	π	1.725	BD*(2)C6-C27	π*	0.298	20.24	0.3	0.07
BD(2)C26-C30	π	1.725	BD*(2)C28-C29	π*	0.377	13.42	0.3	0.06
BD(2)C28-C29	π	1.612	BD*(2)C6-C27	π*	0.298	16.33	0.28	0.062
BD(2)C28-C29	π	1.612	BD*(2)C26-C30	π*	0.415	27.49	0.26	0.078
BD(1)C29-C30	π	1.971	BD*(2)N4-C26	σ*	0.04	5.24	1.04	0.066
BD(2)C31-C32	π	1.72	LP)(1)C8	n	1.025	46.49	0.14	0.09
BD(2)C31-C32	π	1.72	BD*(2)C33-C34	π*	0.225	15.78	0.3	0.063
BD(2)C31-C32	π	1.72	LP)(1)C8	n	1.025	46.49	0.12	0.09
BD(2)C33-C34	π	1.705	BD*(2)C9-N10	σ*	0.442	22.54	0.26	0.07
BD(2)C33-C34	π	1.705	BD*(2)C31-C32	π*	0.269	19.26	0.28	0.066
LP(1)N1	n	1.765	LP*(1)C5	n	0.965	4.32	0.21	0.103
LP(1)N2	n	1.765	BD*(2)C3-N4	σ*	0.643	26.73	0.29	0.89
LP*(1)C5	n	0.965	BD*(2)C3-N4	σ*	0.643	70.97	0.09	0.08
LP*(1)C5	n	0.965	BD*(2)C20-C21	π*	0.351	30.94	0.19	0.08
LP(1)C8	n	1.025	BD*(2)C3-N4	σ*	0.643	5.42	0.01	0.008
LP(1)C8	n	1.025	BD*(2)C7-C12	π*	0.363	62.35	0.13	0.09

(*Contd.*)

Table 3 — Second order perturbation theory analysis of Fock matrix in NBO basis of the title compound (*Contd*.)

Donor (i)	Type	Ed/e	Acceptor (i)	Type	Ed/e	E(2)a	E(j)a-E(i)b	F(I,j)c
LP(1)C8	n	1.025	BD*(2)C9-N10	σ*	0.492	87.47	0.13	0.108
LP(1)C8	n	1.025	BD*(2)C31-C32	π*	0.269	52.87	0.15	0.1
LP(1)N10	n	1.917	BD*(1)C8-C9	π*	0.042	11.22	0.85	0.088
LP*(1)C11	n	0.928	BD*(2)C7-C12	π*	0.363	73.91	0.12	0.102
LP*(1)C11	n	0.928	BD*(2)C9-N10	σ*	0.492	79.68	0.12	0.102
LP*(1)C11	n	0.928	BD*(2)C13-C18	π*	0.392	35.49	0.16	0.081
LP(2)F19	n	1.988	BD*(2)C15-C16	π*	0.028	6.78	0.96	0.072
LP(2)F19	n	1.967	BD*(2)C16-C17	π*	0.027	6.79	0.96	0.072
LP(3)F19	n	1.967	BD*(2)C16-C17	π*	0.37	21.53	0.42	0.091
LP(1)C25	n	1.908	BD*(2)C20-C21	π*	0.351	69.97	0.12	0.095
LP(1)C25	n	1.123	BD*(2)C23-C24	π*	0.301	66.48	0.16	0.109
LP(1)O36	n	1.123	BD*(2)C22-N35	σ*	0.056	6.27	1.2	0.07
LP(2)O36	n	1.979	BD*(2)C22-N35	σ*	0.056	9.29	0.69	0.074
LP(2)O36	n	1.844	BD*(1)N35-O37	σ*	0.125	30.97	0.45	0.106
LP(3)O36	n	1.543	BD*(2)C22-N35	σ*	0.722	54.25	0.21	0.102
LP(2)O37	n	1.87	BD*(2)C22-N35	σ*	0.722	13.34	0.28	0.06
LP(1)O38	n	1.962	BD*(2)C28-C29	π*	0.029	8.27	1.08	0.084
LP(2)O38	n	1.809	BD*(2)C28-C29	π*	0.029	36.86	0.32	0.102
BD*(2)C9-N10	σ*	0.492	BD*(2)C33-C34	π*	0.225	65.93	0.04	0.077
BD*(2)C16-C17	π*	0.37	BD*(2)C14-C15	π*	0.298	231.65	0.01	0.082
BD*(2)C22-N35	σ*	0.722	BD*(2)C20-C21	π*	0.351	76.96	0.07	0.09
BD*(2)C22-N35	σ*	0.722	BD*(2)C23-C24	π*	0.301	37.3	0.11	0.08
BD*(2)C26-C30	π*	0.415	BD*(2)C6-C27	π*	0.298	144.38	0.02	0.078
BD*(2)C26-C30	π*	0.415	BD*(2)C28-C29	π*	0.377	220.85	0.02	0.082
BD*(2)C31-C32	π*	0.269	BD*(2)C33-C34	π*	0.225	146.13	0.02	0.079

significant intramolecular charge transfers in **(3)** are observed from π (C16-C17) to π* (C14-C15), π (C26-C30) to π* (C6-C27), π (C28-C30) to π* (C28-C29) and π (C31-C32) to π* (C33-C34) with stabilization energies of 231.65, 144.38, 220.85 and 146.13 kcal mol^{-1} respectively indicating profound conjugation and delocalisation of electrons from the heteroatom to the π system . Apart from these transitions, other π → π * and n → π * intramolecular transitions are also seen with stabilisation energy values ranging between 20-50 kcal mol^{-1} thus showing delocalisation of electrons within the system.

3.7 Non-linear Optical Analysis

DFT studies are very useful in the analysis of the NLO properties of molecules. The NLO behaviour of any molecule can be studied by determination of its polarizability, dipole moment and first hyperpolarizability values. The non-linear optical properties have applications in various fields as telecommunications, signal processing and optical interconnections etc.[34-36]. The first hyper polarizability of the studied compound **(3)** was computed using the B3LYP/6-31G (d, p) basis set. The overall calculations for total dipole moment μ, the average polarizability α^{tot} and the first hyperpolarizability β^{tot}, were done as per Kleinman symmetry[37]. The corresponding data of electronic dipole moment μi (i = x, y, z), polarizability αij and first order hyperpolarizability βijk are presented in Table S2. As the values of polarizability α=0.005723 a.u. and hyper polarizability β=0.00872248 a.u. as per Gaussian output have been calculated in atomic mass units (a. u.), therefore these are converted into electrostatic units (e.s.u) (α: 1 a. u = 0.1482×10^{-24} esu; β: 1 a.u. = 0.0086393×10^{-30} esu). For a molecule to be NLO candidate, the values of polarizability and dipole moments should be large. The values of partial dipole moment, polarizability and hyperpolarizability which are 8.7693 D, 0.0008470×10^{-24} esu and 0.000075×10^{-30} esu respectively suggested that the molecule can be a NLO material. The presence of π conjugated system and profound delocalisation of electron density over the molecule confirms it non-linearity.

3.8 Thermodynamic Properties

The thermodynamic data furnishes many useful informations as per the relationships of thermodynamic functions according to the second law of thermodynamics in thermo chemical field[38]. Zero-point vibrational energy, rotational temperature and other thermodynamic parameters of the title molecule are presented in Table S3 and S4. Vibrational analysis using DFT/B3LYP was

performed to obtain standard statistical thermodynamic functions, heat capacity (CV) and entropy (S) at various temperatures (100-600 K) for the title molecule. Results indicated that the corresponding increase in standard statistical thermodynamic functions with increasing temperature is due to the progression in molecular vibrational intensities with temperature[39-40]. Fig. 8 contains the correlation graph between the thermodynamic functions.

3.9 Reactivity Descriptors

3.9.1 Global Reactivity Descriptors

The global reactivity descriptors can be very well used for elucidation of a reaction's mechanism and to locate the probable reactive sites in molecules[41]. Global reactivity descriptors as Energies of frontier molecular orbitals (εLUMO, εHOMO), band gap (εLUMO-εHOMO), ionization potential (IP), electron affinity (EA), electronegativity (χ), global hardness (η), chemical potential (μ), global electrophilicity index (ω) and global softness (S) for the title compound, are listed in Table 4. The negative chemical potential of the title compound with a value of -0.1448 clearly indicated its stability.

3.9.2. Local Reactivity Descriptors

The contribution of every single atom to the molecule can be obtained by the condensed value around each atomic site. The susceptibility of a particular site to nucleophilic or electrophilic attack can be observed with the help of maximum values of local reactivity descriptors[42-43]. Table 5 contains the values for condensed Fukui functions, softnesses and electrophilicity indices for specific atomic sites of the title molecule. The corresponding enhancement in the values of Condensed Fukui functions, softness, electrophilicity indices represented by fk+, sk+, ωk+, evident at C34, N35, O36, O37 and O38 indicated that these sites are more liable to nucleophilic attack. On the other hand, the increased values of fk-, sk-, ωk- at C13, C18, C21 and C30 suggested the susceptibility of the electrophilic attack on these sites of the molecule.

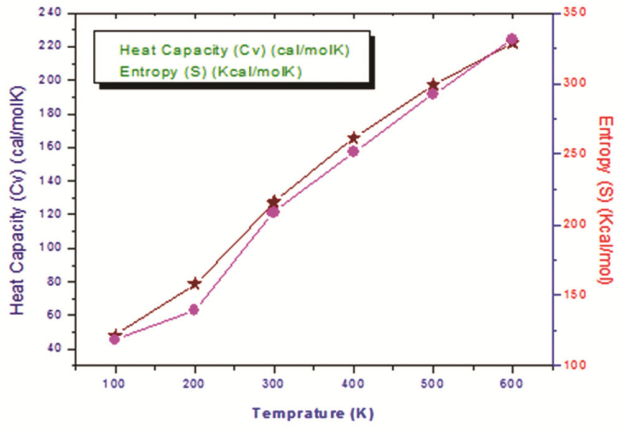

Fig. 8 — Correlation graph between thermodynamic functions

4 Biological Evaluations

4.1 Antimicrobial Screening

Disc diffusion method was employed to find out the zone of inhibition of compounds. Micro broth dilution method was used to determine MIC values of compounds as per described method of Vipra et al. using 96 well plates[44]. The title compound 3 was screened against one Gram positive [Staphylococcus aureus (Sa) MTCC 96], and three Gram negative [Pseudomonas aeruginosa (Pa) MTCC 741, Salmonella typhi (St) MTCC 537, Escherichia coli (Ec) MTCC 1304] bacteria using Erythromycin (E) as the standard antibacterial drug. The compound was further screened for its antifungal activity against one fungal species [Candida albicans (Ca) MTCC 184] where Fluconazole was used as the standard antifungal agent. The results obtained from biological screening of the title compound, clearly indicated in Table 6(a) and Fig. 9, revealed that the compound is biologically active against S. typhi with MIC value of 200 μg/mL and diameter of zone of inhibition as 10 mm which is quite comparable to the standard drug Erythromycin (MIC=200 μg/mL, ZOI=12mm). It was also observed that the compound showed no significant activity against the other tested bacterial and fungal strains. The biological activity displayed by the compound against S. typhi can be attributed to the presence of two electron withdrawing substituents (-F, -NO_2) which might render a better fit into the receptor site.

4.2 Antioxidant Activity

Antioxidant properties of the title compound were investigated by 2,2-diphenyl-1-picrylhydrazyl (DPPH)

Table 4 — Calculated ε_{LUMO}, ε_{HOMO}, energy band gap $\varepsilon_{LUMO}-\varepsilon_{HOMO}$, ionization potential (IP), electron affinity (EA), electronegativity (χ), global hardness (η), chemical potential (μ), global electrophilicity index (ω), global softness (S) and additional electronic charge (ΔN max) in eV for assayed compound, using DFT/B3LYP/6-31G(d, p).

ϵ_H	ϵ_L	ϵ_H-ϵ_L	I	A	χ	η	μ	ω	S
-0.1551	-0.1346	-0.0104	0.1551	0.1346	0.1448	-0.0204	-0.1448	0.0724	-0.0102

Table 5 — Fukui functions (fk^+, fk^-), local softnesses (sk^+,sk^-) in eV, local electrophilicity indices (ωk+, ωk-) in eV for specific atomic sites of molecule.

	q_N	q_N+1	q_N-1	f_k+	f_k-	sk^+	sk^-	ωk^+	ωk^-
1N	-0.0620	-0.0242	-0.0778	0.0378	0.0158	0.000386	0.000161	0.00275	0.00114
2N	-0.0123	0.008037	-0.04709	0.020344	0.034783	0.000207	-0.00035	0.001472	0.00251
3C	0.353557	0.417564	0.321654	0.064007	0.031903	0.000652	-0.00032	0.004637	0.00230
4N	0.615252	0.588383	0.616536	0.026869	0.001284	-0.00027	-1.309	0.001916	9.296
5C	0.425066	0.485518	0.435508	0.060452	0.010442	-0.00061	0.00010	0.004376	0.00075
6C	0.004902	0.010358	0.016597	0.01526	0.011695	-0.0005	-0.00011	0.001104	0.00084
7C	0.062191	0.068884	0.049771	0.006693	0.01242	-6.00653	-0.00012	0.00043	0.00089
8C	0.022325	0.003154	0.033385	0.019171	0.01106	-0.0009	0.000112	0.001388	0.00080
9C	0.298477	0.307103	0.292733	0.008626	0.005744	-8.245	-5.8555	0.000624	0.0004
10N	0.622825	0.577477	0.659604	0.045348	0.036779	-0.00046	-0.0003	0.003283	0.002
11C	0.220708	0.228261	0.212001	0.007553	0.008707	-7.45 5	-8.8881	0.000547	0.00063
12C	0.075172	-0.02949	0.106689	0.045682	0.031517	-0.00046	-0.00032	0.00337	0.00228
13C	0.056396	0.056135	0.056617	0.000261	0.000221	2.6622	2.25452	-1.1.88	-1.6005
14C	0.004418	0.017075	0.008952	0.012657	0.01337	0.000129	-0.00013	0.00091	0.0009
15C	-0.05627	-0.02749	0.080855	0.02878	0.024585	0.000293	-0.00025	0.0020	0.00177
16C	0.34025	0.35646	0.325663	0.01621	0.014587	-0.00016	-0.00014	0.00117	0.00105
17C	0.049003	0.021594	0.072204	0.027409	0.023201	-0.00027	-0.0002	0.00198	0.0016
18C	0.000772	0.000776	0.000051	0.00406	0.000721	-4.008	-7.356	2.897	5.220
19F	0.293082	0.277406	0.306128	0.015676	0.013046	-0.00015	-0.00013	0.001132	0.000
20C	0.102893	0.103841	0.10649	0.000948	0.003597	-9.6696	3.6405	6.6.8605	0.00026
21C	0.034438	-0.02028	0.031942	0.014158	0.002496	-0.00014	2.54592	0.001025	-0.000
22C	0.298688	0.298468	0.286506	-0.00022	0.012182	2.244	-0.00012	-1.505	0.0008
23C	0.053651	0.047221	0.166377	0.100872	0.112726	-0.0010	-0.00114	0.00733	0.0081
24C	0.001722	0.036178	0.048948	0.034456	0.05067	0.000351	-0.00051	0.002494	0.00366
25C	0.056513	0.012846	0.170725	0.043667	0.114212	0.000445	-0.00116	0.00316	0.00826
26C	0.173954	0.147731	0.191196	0.026223	0.017242	0.000267	0.00017	-0.0018	0.00124
27C	0.032308	0.000915	0.049847	0.031393	0.017539	-0.00032	-0.00017	0.002273	0.00126
28C	0.356613	0.365963	0.358379	0.00935	0.001766	-9.537	1.8013	0.00064	0.00012
29C	0.012708	0.013816	-0.02571	0.026524	0.013002	-0.0002	-0.0001	0.00192	0.0009
30C	0.020918	0.025183	0.027489	0.004265	0.006571	-0.00004	6.70242	0.000306	-0.000
31C	0.094937	0.080943	0.112818	0.013994	0.017881	0.000142	-0.00018	0.00106	0.00129
32C	0.071348	0.000299	0.136496	0.071647	0.065148	-0.00073	-0.0006	0.0051	0.00471
33C	0.005723	0.040323	-0.04651	0.046046	0.040787	-0.00046	-0.00041	0.0033	0.00295
34C	0.206778	0.075752	0.046409	0.131026	0.253187	0.00133	-0.00258	-0.00948	0.01833
35N	0.418864	0.222031	0.171515	0.640895	0.590379	-0.00653	0.00602	0.04648	-0.0427
36O	0.089509	-0.40259	0.542186	0.313081	0.452677	0.00319	-0.00461	-0.0226	0.0327
37O	0.529953	0.047085	0.153105	0.482868	0.376848	-0.00492	0.0038	0.03493	-0.0272
38O	0.276106	0.515458	-0.54143	0.791564	0.817536	0.00807	-0.00833	-0.0573	0.05918
39C	0.276106	0.29635	0.262866	0.020244	0.01324	-0.00020	-0.00013	0.00146	0.00095

Table 6(a) — *In-vitro* antimicrobial activity of compounds 8 MIC, μg/mL and diameter of zone of inhibition against different strains.

Compound	*Bacteria*				*Fungi*
	Gram positive		*Gram negative*		
	S. aureus	*P. aeruginosa*	*S. typhi*	*E. coli*	*C. albicans*
3	200 (10)	400 (7)	200 (10)[a]	200 (11)	400 (7)
E	0.19 (32)	50 (20)	200 (12)	<6.25 (15)	-
Fl	-	-	-	-	6.25 (21)

(-) No activity observed.

[a]Entries in bold font indicates excellent activity than reference drug Erythromycin (E) and Fluconazole (Fl).

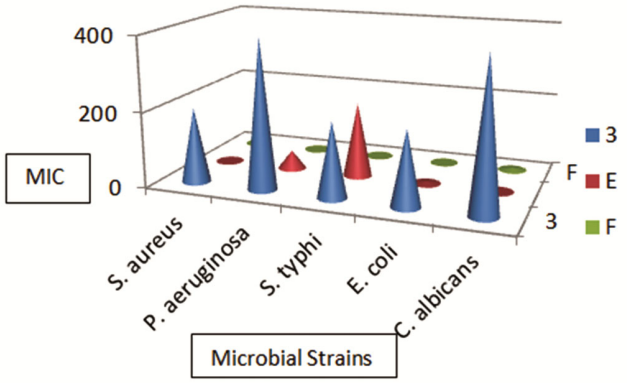

Fig. 9 — *In-vitro* antimicrobial evaluation against bacterial strains and fungal strain

Table 6(b) — Antioxidant activity of compound 3

S. No.	Compound	Percentage of inhibition(%)
1	3	89

assay[45]. The results of antioxidant activity are reported in Table 6(b). DPPH in its stable form (nitrogen centered free radical) with dark color has absorbance maxima at 350 nm and 517 nm. However, when it is reduced to its non-radical form by the action of antioxidant, its absorbance is sharply reduced at 517 nm resulting in colorless solution. The title compound displayed a positive antioxidant activity as depicted by reduction in color during the reaction with percentage inhibition of 89%.

5 Conclusions

The present work involves detailed structural elucidation, characterization, antimicrobial and antioxidant evaluation of 2-(4-fluorophenyl)-4-(4-(4-methoxyphenyl)-5-(3-nitrophenyl)-4H-1,2,4-triazol-3-yl)quinoline (3). DFT studies revealed that a good correlation is seen in theoretical and experimental chemical shift values for both ^{1}H and ^{13}C NMR. Also the vibrational bands ascertained in the FT-IR spectrum have wave numbers lying in the expected range. The potentially reactive sites of the title compound were investigated by electrostatic potential surfaces (ESP). Reactivity descriptors were used to ascertain the nucleophilic (C34, N35, O36, O37, O38) and electrophilic centres (C13, C18, C21 and C30) in the molecule. The values of partial dipole moment and polarizability put forward candidacy of the molecule as an NLO material. A corresponding increase was seen in thermodynamic parameters with the rise in the temperature. Along with it, natural bond orbital (NBO) analysis depicted hyper conjugative interactions and electron delocalization within the molecule. The results obtained from biological screening of the title compound clearly indicated that the compound is biologically active against *S. typhi* with MIC value of 200 µg/mL and diameter of zone of inhibition as 10 mm which is quite comparable to the standard drug Erythromycin (MIC=200 µg/mL, ZOI=12mm). It was also observed that the compound showed no significant activity against the other tested bacterial and fungal strains. The biological activity displayed by the compound against *S. typhi* can be attributed to the presence of two electron withdrawing substituents (-F, -NO_2) which might render a better fit into the receptor site. The title compound displayed a positive antioxidant activity as depicted by reduction in color during the reaction with percentage inhibition of 89%.

Conflict of interest

The authors declare that they have no conflict of interest.

Supplementary Material

The comparison of calculated and optimised structural parameters, dipole moment, polarizability, first order hyperpolarizability, calculated thermodynamic parameters and thermodynamic functions, along with ^{1}H-NMR, ^{13}C-NMR mass and IR spectra of compound 3 are provided as supplementary material.

Acknowledgement

The authors express their sincere gratitude to the Head, Department of Chemistry, Lucknow University, Lucknow, for providing laboratory facilities and cluster facilities for computational work. Authors are also thankful to the Director, CDRI, Lucknow for spectral analysis.

References

1 Ventura M C, Kassab E, Buntinx G & Poizat, *Phys Chem Chem Phys*, 2 (2000) 4682.
2 Shin D N, Hahn J W, Jung K H & Ha T K, *J Raman Spectrosc*, 29 (1998) 245.
3 Giese B & Naughton D Mc, *Phys Chem Chem Phys*, 4 (2002) 5161.
4 Parr R G & Yang W, *Density functional theory of atoms and molecules*, Oxford University Press, New York, 1989.
5 Praveena C H L, Rani V E, Spoorthy Y N & Ravindranath L K, *J Chem Pharm Res*, 5 (2013) 280.
6 Shah P J, Patel H S & Patel B P, *J Saudi Chem Soc*, 17 (2013) 307.
7 Zonios D I & Bennett D, *Care Med*, 29 (2008) 198.

8 Dismukes W E, *Clin Infect Dis*, 30 (2000) 653.
9 Finar I L, *Organic Chemistry: Stereochemistry and the Chemistry of Natural Produc*t, 2 (1962) 621.
10 Varvarason A, Kakoulidou A T, Papastasikoudi S & Tiligada E, *Arzneim Forsch*, 50 (2000) 48.
11 Gokce M, Cakir B, Earl K & Sahin M, *Arch Pharm*, 334 (2001) 279.
12 Pintilie O, Profire L, Sunel V, Popa M & Pui A, *Molecules*, 12 (2007) 103.
13 Zhou X J, Lai L H, Ji G Y & Zhang Z X, *J Agric Food Chem*, 50 (2002) 3757.
14 Chem H, Li Z & Han Y, *J Agric Food Chem*, 48 (2000) 5312.
15 Passannanti A, Diana P, Barraja P, Mingoia F, Lauria A & Cirrincione G, *Heterocycles*, 48 (1998) 1229.
16 Hosur M C, Talwar M B, Bennur R S, Benur S C, Patil P A & Sambrekar S, *Ind J Pharm Sci*, 55 (1993) 86.
17 Udupi R H, Kulkarni V M, Purushottamachar P & Srinivasalu N, *J Indian Chem Soc*, 79 (2002) 381.
18 Mhasalkar M Y, Shah M H, Nikam S T, Anantanarayanan K G & Deliwala C V, *J Med Chem*, 14 (1971) 260.
19 Mullican M D, Wilson M W, Connor D T, Schrier D J & Dyer R D, *J Med Chem*, 36 (1993) 1090.
20 Mhasalkar M Y, Shah M H, Nikam S T, Anantanarayanan K G, Deliwda C V, *J Med Chem*, 13 (4) 672.
21 Frisch M J, Trucks G W, Schlegel H B, Scuseria G E, Robb M A, Cheeseman J R, Scalmani G, Barone V, Mennucci B, Petersson G A, Nakatsuji H, Caricato M, Li X, Hratchian H P, Izmaylov A F, Bloino J, Zheng G, Sonnenberg J L, Hada M, Ehara M, Toyota K, Fukuda R, Hasegawa J, Ishida M, Nakajima T, Honda Y, Kitao O, Nakai H, Vreven T, Montgomery Jr J A, Peralta J E, Ogliaro F, Bearpark M, Heyd J J, Brothers E, Kudin K N, Staroverov V N, Kobayashi R, Normand J, Raghavachari K, Rendell A, Burant J C, Iyengar S S, Tomasi J, Cossi M, Rega N, Millam J M, Klene M, Knox J E, Cross J B, Bakken V, Adamo C, Jaramillo J. Gomperts R., Stratmann R E, Yazyev O, Austin A J, Cammi R, Pomelli C, Ochterski J W, Martin R L, Morokuma K, Zakrzewski V G, Voth G A, Salvador P, Dannenberg J J, Dapprich S, Daniels A D, Farkas O, Foresman J B, Ortiz J V, Cioslowski J, Fox D J, Gaussian-09, Revision A.02. Gaussian, Inc., Wallingford CT, 2009.
22 Schlegel H B, *J Comput Chem*, 3 (1982) 214.
23 Chaitanya K, Santhamma C, Prasad K & Veeraiah V, *Journal of Atomic and Molecular Sciences*, 3 (2012) 1.
24 Holla B S, Poojary K N, Poojary B, Bhat K S, Kumari N S, *Indian J Chem*, 44 (2005) 2114.
25 Lutz R, Bailey P, Clark M, Codington J, Deinet A, Freek J, Harnert G, Leake N, Martin T, Rowlett R, Salsbury J, Shearer N, Smith J & Wilson J, *J Am Chem Soc*, 68 (1946) 1813.
26 Hoi N P B, Royer R, Xuong N D & Jacquignon P, *J Org Chem*, 18 (1953) 1209-1224.
27 Olasunkanmi L O, Ige J & Ogunlusi G O, *J Chem*, (2013) 1.
28 Patel U H, Gandhi S A, *J Pure & Appl Phys*, 49 (2011) 263.
29 Schuchardt K L, Didier B T, Elsethagen T, Sun L, Gurumoorthi V, Chase J, Li J & Windus T L, *J Chem Inf Model*, 47 (2007) 1045.
30 Politzer P & Murray J S, *Theoretical biochemistry and molecular biophysics: A comprehensive survey*, in D. L. Beveridge, R. Lavery Eds., 1991.
31 Gupta V P, Sharma A, Virdi V, Ram V J, *J Spectrochim Acta*, 64 (2006) 57.
32 Glendening E D, Reed A E, Carpenter J E & Weinhold F, NBO Version 3.1, TCI, University of Wisconsin, Madison, 1998.
33 Reed A E, Curtis L A & Weinhold F, *Chem Rev*, 88 (1988) 899.
34 Andraud C, Brotin T, Garcia C, Pelle F, Goldner P, Bigot B & Collet A, *J Am Chem Soc*, 116 (1994) 2094.
35 Nakano M, Fujita H, Takahata M & Yamaguchi K, *J Am Chem Soc*, 124 (2002) 9648.
36 Geskin V M, Lambert C & Bredas J L, *J Am Chem Soc*, 125 (2003) 15651.
37 Kleinman D A, *Phys Rev*, 126 (1962) 1977.
38 Zhang R, Du B, Sun G & Sun Y, *J Spectrochim Acta*, 75 (2010) 1115.
39 Ott J B & Goates J B, *Calculations from statistical thermodynamics*, Academic Press, 2000.
40 Sajan D, Josepha L, Vijayan N & Karabacak M, *J Spectrochim Acta*, 81 (2011) 85.
41 Fleming I, *Frontier Orbitals and Organic Chemical Reactions*, John Wiley and Sons, New York, 1976.
42 Parr R G, Szentpaly L & Liu S, *J Am Chem Soc*, 121 (1999) 1922.
43 Chattaraj K & Giri S, *J Phys Chem A*, 111 (2007) 11116.
44 Vipra A, Desai S N, Junjappa R P, Roy P, Poonacha N, Ravinder P, Sriram B & Padmanabhan S, *Adv Microbiol*, 3 (2013) 181.
45 Gangwar M, Gautam M K, Sharma A K, Tripathi Y B, Goel R K & Nath G, *The Sci World J*, (2014) 1.